[Short title + Author Name - P&H title] 17 (2024) 105977

Contents lists available at ScienceDirect

Arabian Journal of Chemistry

journal homepage: www.ksu.edu.sa

Experimental study on inhibiting methane-coal dust explosion by APP-diatomite composite explosion suppressant in the pipe network

Jinzhang Jia , Xiuyuan Tian *

College of Safety Science and Engineering, Liaoning Technical University, Fuxin 123000, China
Key Laboratory of Thermal Dynamic Disaster Prevention and Control of Ministry of Education, Liaoning Technical University, Hulu Dao, Liaoning 125105, China

ARTICLE INFO

Keywords:
Safety engineering
Pipe network
Methane/coal dust explosion
Composite suppressant
Explosive residue

ABSTRACT

To prevent and control the methane/coal dust compound explosion disaster, the APP-diatomite composite powder inhibition of methane/coal dust compound explosion experiments were carried out in the self-constructed pipe network. The composite powder was characterized by scanning electron microscopy and X-ray photoelectron spectroscopy. The change rules of methane/coal dust composite explosion pressure and flame propagation velocity were analyzed using different compounding ratios of powders in several monitoring points. The results show that the composite powder exhibited irregular morphology and the APP powder is uniformly distributed on the diatomite porous mesh structure. When the APP loading on the surface of diatomite is 40 wt%, composite powder has the best effect on explosion suppression, with the peak maximum explosion overpressure and the peak maximum flame propagation velocity reduced by 71.5 % and 92.2 %, respectively. The explosion suppression mechanism is revealed through pyrolysis properties, explosion products, and chain reaction.

1. Introduction

Methane-coal dust mixture explosions can reach a detonation state in a very short time, and the lives of underground personnel are jeopardized (Shi et al., 2023; Yu et al., 2023; Moiseeva et al., 2023). For example, on 11 March 2024, a large gas explosion occurred at the Xieqiao coal mine of Huaihe Energy Holding Group Co., Ltd. in Anhui Province, resulting in 9 deaths and 15 injuries. On 21 August 2023, a major gas explosion occurred at the Xintai coal mine in Yanchuan County, Yan'an, Shaanxi Province, resulting in 11 deaths and 11 injuries. Underground suspended coal dust volatilizes a large number of combustible gases and adheres around the coal dust when the gases gather to a certain concentration and absorb a large amount of heat, a chain reaction will occur, and the heat released from oxidation will cause the coal dust particles to flash fire, and when it reaches a certain level, it will increase the power of the methane explosion (Hou et al., 2023; Gieras et al., 2015; Di et al., 2023; Dunn-Rankin et al., 2000; Pearce et al., 2023). Ajrash et al. (2016) conducted methane/coal dust explosion experiments in a large cylindrical pipe and concluded that when 30 g/m^3 of coal dust was added to 6 vol% methane/air, the explosion pressure increased nearly twofold. The risk of a methane/coal dust explosion in a 20L spherical explosion vessel is much higher than that of a coal dust explosion. Methane concentration, coal dust concentration, and initial pressure all had a significant effect on the mixed explosion (Song et al., 2019). Zhao et al. (2020) conducted explosion tests on coal dust in a combustible gas (CH_4, H_2, CO) environment. The results showed that the explosion pressure increased with the increase of combustible gas concentration, and the explosion risk of adding methane was found to be higher than the other two combustible gases. The above study confirms that a methane/coal dust mixture explosion is more hazardous than a single-phase explosion.

The development of high-performance, environmentally friendly detonation suppressants is the main research goal in the direction of methane-coal dust detonation suppression. Blast suppressant properties and materials have an impact on the effect of blast suppression and reaction mechanisms. Currently, the study of explosion suppression materials includes inert gas suppressants (Zhao et al., 2021; Wang et al., 2022; Zhao et al., 2023), fine water mist suppressants (Cao et al., 2024; Cao et al., 2023; Jiang et al., 2022), powder suppressants (Zhao et al., 2021; Zhao et al., 2022a; Dai et al., 2022; Yu et al., 2024; Guo et al., 2024) porous materials suppressants (Sun et al., 2011; Long et al., 2022; Duan et al., 2022), halogenated hydrocarbons (Dong et al., 2022) and so on. Among them, the powder inhibitor compared to other types of explosion suppression media with portable, easy-to-store-to-store, and

* Corresponding author at: College of Safety Science and Engineering, Liaoning Technical University, Fuxin 123000, China.
E-mail addresses: jiajinzhang@lntu.edu.cn (J. Jia), 1406784586@qq.com (X. Tian).

https://doi.org/10.1016/j.arabjc.2024.105977
Received 20 May 2024; Accepted 20 August 2024
Available online 30 August 2024

cost-effective advantages, so the choice of powder inhibitor as a detonation inhibitor has become a hot spot in recent years.

For example, Zhao et al. (2022b) investigated the suppression characteristics and mechanism of APP powder on the methane/coal dust composite deflagration flame in a vertical combustion pipe, and the experimental results showed that the addition of APP powder effectively suppressed the flame propagation, flame velocity and temperature of the methane/coal dust explosion Wei et al. (2021) and others used NaY zeolite as a carrier, modified by iron ions, and combined with ammonium polyphosphate (APP) to prepare a new composite inhibitor to explore the explosion suppression performance of the new APP/NaY-Fe inhibitor. The results showed that the iron ion modification can effectively improve the explosion suppression performance of the material. When adding 50 wt% inhibitor, the maximum explosion pressure of coal dust was reduced to 0.13 MPa. Yuan et al. (2021) used a 20 L spherical explosive device to carry out porous minerals, APP, and its composite powders in different compositions, and different additive concentration conditions of methane explosion suppression test, the experimental results showed that the synergistic inhibition effect of the composite powder on methane explosion was most significant when the powder addition was 0.100 g/L and the mass composition ratio of porous minerals to APP was 1:3. The above studies showed that ammonium polyphosphate (APP) had good detonation suppression properties, and the APP powder and porous materials compounded powder detonation suppression performance was significantly improved.

Diatomite, a green, non-toxic explosion suppression material, with a porous structure, porosity of 90–92%, with a large specific surface area, its microporous structure and surface hydroxyl features are the key factors affecting the effect of its suppression of explosives. However, a single diatomite had a limited ability to suppress detonation (Cheng et al., 2010). He et al. (2022) and others analyzed the microscopic mechanism of gas explosion inhibition by diatomite based on quantum chemical theory, and the results showed that the congenic silanols in diatomite possess a better inhibition effect compared with isolated silanols. Luo et al. (2016) and others explored the inhibition effect of diatomite powder aerosol on gas explosion, and the results showed that, due to the unique porous structure of diatomite its explosion suppression effect is mainly dependent on weakening the activity of free radicals, adsorption of free radicals in the explosion reaction.

Therefore, in this paper, ammonium polyphosphate (APP) is compounded with diatomite to produce APP-diatomite compounded powder, so that the diatomite in the compounded powder not only makes up for the defects of APP without porosity and improves the phenomenon that monomer APP easily agglomerated and adhered to, but also makes the compounded powder with the characteristics of strong adsorption capacity in diatomite. To investigate the effect of APP and diatomite compounded explosion suppressant on the explosion characteristics of methane/coal dust mixture in the pipeline network.

In addition, methane/coal dust mixture explosion has certain specificity and complexity, previous research mainly focuses on single-section long straight pipeline, spherical explosion tanks, and other closed containers to carry out experimental research to inhibit the methane/coal dust mixture explosion, this kind of experimental containers and the actual pipeline path correlation is not close enough. Therefore, this paper carried out the experimental study on the inhibition of methane/coal dust mixture explosion by different compound ratios of APP-diatomite in the pipe network with bifurcated pipeline and right-angle pipeline and analyzed the inhibition characteristics and inhibition mechanism of APP-diatomite compound ratio on the propagation of shock wave and flame wave of methane/coal dust mixture explosion. To provide technical guidance and theoretical support for the management of mixed gas and coal dust explosions.

2. Experiment

2.1. Experimental apparatus

As shown in Fig. 1, the experimental setup consists of an experimental pipe network system, dynamic data acquisition system, powder spraying system, and ignition system. The experimental piping system consists of several carbon steel pipes with different lengths and inner diameters of 300 mm, each of which is connected by flanges. The size of the pipe network is 4500 mm × 3600 mm, the volume of the explosion chamber is 30 L, the explosion chamber is separated from the pipe connection by polytetrachloroethylene film, and the maximum pressure resistance of the pipe network is 2.5 MPa. The two outlets of the pipe network are closed with flanges as well as a PTFE membrane for explosion relief. The pipe is equipped with several sensor sockets of size M20 x 1.5 for simultaneous insertion of pressure sensors, temperature sensors, and flame sensors. The various components are connected to the piping using female threads, and the airtightness of the unit is improved by installing silicone gaskets at the connection between each component and its corresponding piping. The dynamic data acquisition system mainly includes a QSY8124 pressure sensor (range: 0–10 MPa), NANMAC transient temperature sensor (range: 0–2000 K), CKG100 light-sensitive high-precision flame sensor, and TST6300 dynamic data acquisition instrument. The response times of the pressure sensor, temperature sensor, and flame sensor were 1 ms, 10 ms, and 1 ms, respectively, and the accuracy of the data acquisition device was 0.2 % FS with a continuous acquisition frequency of 10 KHz/CH. The powder spraying system utilizes the gas storage cylinder to provide the driving gas N_2 and the air pump to control the powder spraying pressure. The ignition system mainly includes a DX-GDH high-energy igniter, high-energy spark plug, high-voltage and high-temperature-resistant cable, power supply cable, and external trigger device. The ignition control box is connected to the external trigger wire. The spark plug is placed at the front of the explosion chamber, with an ignition voltage of about 2200 V and a single energy storage of 30J. Let the distance between two flame sensors be L. Record the flame wave passing through two neighboring sensors at different moments t_1 and t_2, then the flame propagation speed is calculated using $v = \frac{L}{t_2 - t_1}$.

2.2. Experimental conditions

Set APP relative to diatomite mass fraction of 25 %, 30 %, 35 %, 40 %, and 45 % for methane-coal dust composite explosion suppression experiments (Liu et al., 2023). The methane concentration was set to 9.5 %, the Daltonton partial pressure method was used for gas distribution, and after compounding, the mass concentration of the composite detonation inhibitor was set to 0.0625 g/L, and the mass concentration of coal dust was 0.125 g/L (Guo et al., 2024). Coking coal with an explosion index of 31.56 % in the Sihe Coal mine was selected as a coal sample in this experiment. Through electron microscope scanning and industrial analysis, the moisture, ash, and volatile content of the coal dust sample are 1.56 %, 12.06 %, and 30.06 %, respectively. The particle size distribution of coal dust is shown in Fig. 2.

2.3. Experimental process

Before each test, the powder is evenly placed at the bottom of the pipeline (see Fig. 1b), the explosion chamber is separated from the pipeline with a polytetrachloroethylene film, and then the explosion chamber is vacuumed and gas test gas with a volume fraction of 9.5 % is injected. There is normal pressure air in the pipeline, after the completion of the gas distribution, the air inlet and the burst outlet are closed at the same time. After standing for 30 s, the air pump is opened, the driving gas N_2 in the gas storage tank is rapidly ejected, and the explosion suppressive powder in the pipeline is blown up. After a

(a) Pipe network diagram.

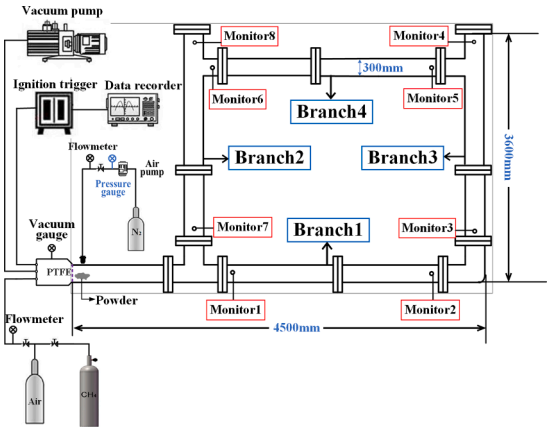

(b) Pipe network schematic diagram.

Fig. 1. Experimental pipe network system.

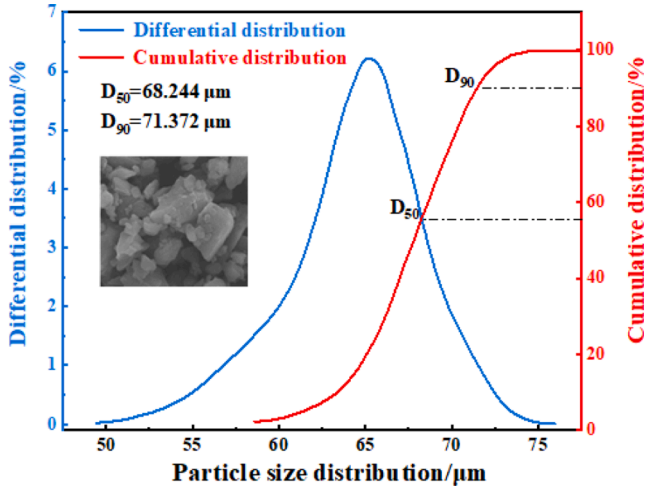

Fig. 2. Particle size distribution and SEM image of pulverized coal.

stationary period of 600 ms, turn on the switch of the external trigger device, and ensure that the igniter and the data acquisition system start to work simultaneously. After the signal light on the device, press the trigger button on the external trigger device to trigger the ignition. After the end of the experiment, the exhaust gas in the pipeline will be discharged, the gas washing work will be carried out in the pipeline, and the next test will be carried out after completion.

2.4. Powder characterization

Fig. 3 shows the electron microscope scanning images of APP, diatomite, and composite powder. From Fig. 3b, it can be seen that diatomite as the carrier of the composite inhibitor showed a disc shape, with fine circular pores distributed on the surface of the disc the pore distribution was more uniform, and the porosity was more developed. As can be seen in Fig. 3c, the crystal structure of the composite powder was highly similar to the structure of diatomite, but its surface was partially covered by APP particles, making its morphology irregular. In the process of explosion suppression, the pores on the surface of the diatomaceous earth not covered by APP particles can adsorb coal dust, free radicals, and so on. Diatomite in the composite powder not only made up for the defects of APP without pores but also improved the phenomenon that monomer APP is easy to agglomerate and stick.

The XRD spectra of diatomite, APP, and diatomite-APP are shown in Fig. 4. The XRD characteristic diffraction peaks of the composite

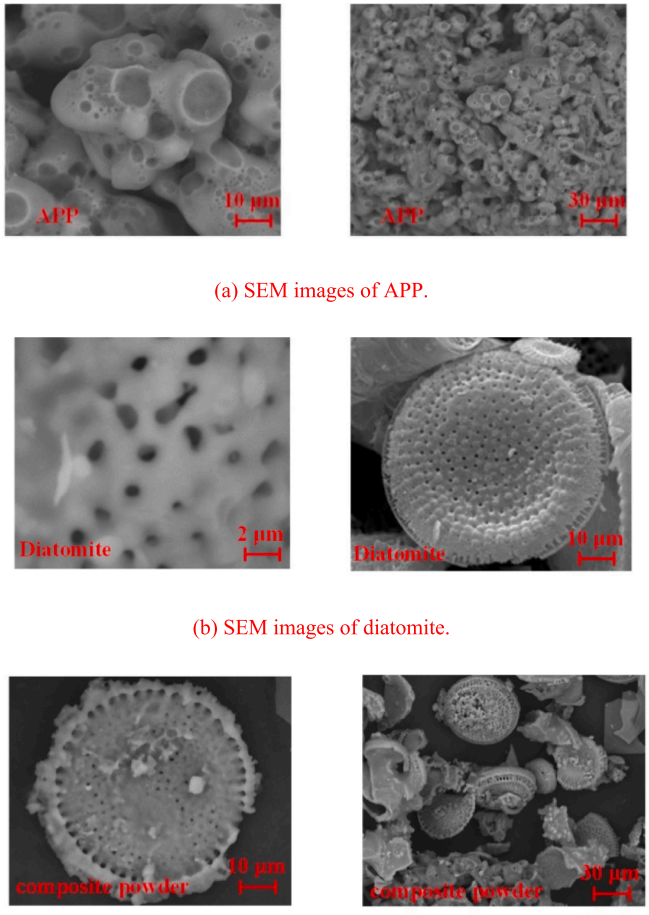

(a) SEM images of APP.

(b) SEM images of diatomite.

(c) SEM images of composite powder.

Fig. 3. SEM images of (a) APP, (b) diatomite, and (c) APP/diatomite composite powder.

powders were basically the same as those of diatomite, and the characteristic diffraction peaks of APP can be observed at 2θ of 14.404°, 16.736°, 18.384°, 20.124°, and 45.578°, respectively. The results of the study show that the composite powder contained diatomite and APP.

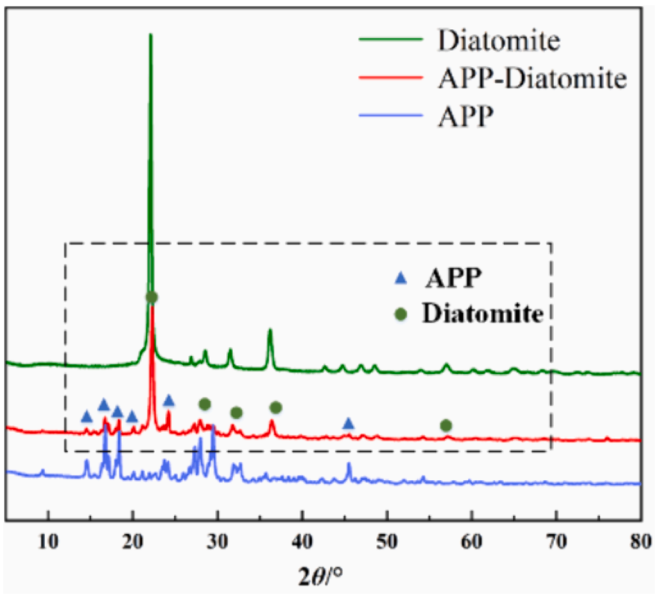

Fig. 4. XRD patterns of explosion inhibitors.

3. Experimental results

3.1. Explosion overpressure

The use of a self-constructed test pipe network to test the single APP, a single diatomite, and different loadings of composite explosion suppression of the monitoring points of the effect of explosion suppression.

Fig. 5 shows the inhibition effect of inhibitors with different compounding ratios on explosion overpressure in monitoring point 1 and monitoring point 2. As shown in Fig. 5a and b, in the absence of explosive suppressants, the influence of complex pipelines, monitoring point 1 and monitoring point 2 of the blank group of overpressure shock waves in the propagation process of both multiple superposition and attenuation. The first overpressure peak at both monitoring points appeared at the beginning of the reaction, with the thermal decomposition of the raised coal dust cloud under the action of high temperature and high pressure, a sufficient amount of combustible gases were generated and participated in the reaction, the overpressure value increased again, and the second overpressure peak appeared, and the second overpressure peak was significantly larger than the first overpressure peak, indicating that the secondary explosion of methane and coal dust occurred in the branch pipe 1 (Zhao et al., 2021). The violent reaction accumulated mainly in the early stages of the explosion, with minor fluctuations in the later stages mainly due to the influence of the reverse overpressure shock wave in the other lines.

After adding the explosion suppressant, monitoring point 1 and monitoring point 2 in the secondary explosion of coal dust and methane characteristics disappear, the overpressure time curve has become “single peak” characteristics, and the overpressure time curve is more gently fluctuating. Overpressure decreased significantly and peak time reached a significant increase in about 1.7 s overpressure down to 0 MPa, the end of the explosion suppression reaction. The overpressure time curve into a “single peak” was mainly due to the suppression of the explosion suppression agent to inhibit the second explosion of methane and coal dust reaction, in the process of suppression of explosion suppression in the explosion suppression powder diluted coal dust and oxygen concentration, so that the coal dust did not reach the conditions of the second explosion. The overpressure time curve of monitoring point 2 after the suppression of explosion fluctuations was slightly larger than the degree of fluctuation of monitoring point 1, mainly due to the location of monitoring point 2 was backward, more sensitive to the impact of the reverse overpressure shock wave than the monitoring point 1.

A comparison of the addition of single-component explosion suppressant found that the addition of APP overpressure peak was slightly smaller than the addition of diatomite overpressure peak, and the addition of APP overpressure peak came later than diatomite explosion suppressant, composite powder overpressure peak was lower than single-component explosion suppressant. In monitoring point 1, the peak overpressure of 25 wt%, 30 wt%, 35 wt%, 40 wt%, and 45 wt% of the compounded explosion suppressant was 0.248 MPa, 0.227 MPa, 0.218 MPa, 0.207 MPa, 0.211 MPa, respectively. Compared to the first overpressure peak without detonation suppressant, the decrease was 49.7 %, 54.0 %, 55.8 %, 58.1 % and 57.2 %, respectively. In monitoring point 2, the peak overpressure of 25 wt%, 30 wt%, 35 wt%, 40 wt%, and 45 wt% of the compounded explosion suppressant was 0.209 MPa, 0.201 MPa, 0.194 MPa, 0.173 MPa, 0.183 MPa, respectively. Compared to the first overpressure peak without detonation suppressant, the decreases was 55.2 %, 56.9 %, 58.4 %, 62.9 %, 60.7 %, respectively. Therefore, the 40 wt% loading rate of the compound explosive suppressant overpressure peak in monitoring point 1 and monitoring point 2 of the largest decline, the best effect of suppressing overpressure shock wave.

Fig. 6 shows the inhibition effect of inhibitors with different compounding ratios on explosion overpressure in monitoring point 3 and monitoring point 4.

As shown in Fig. 6c and d, in the absence of a suppressant, the time

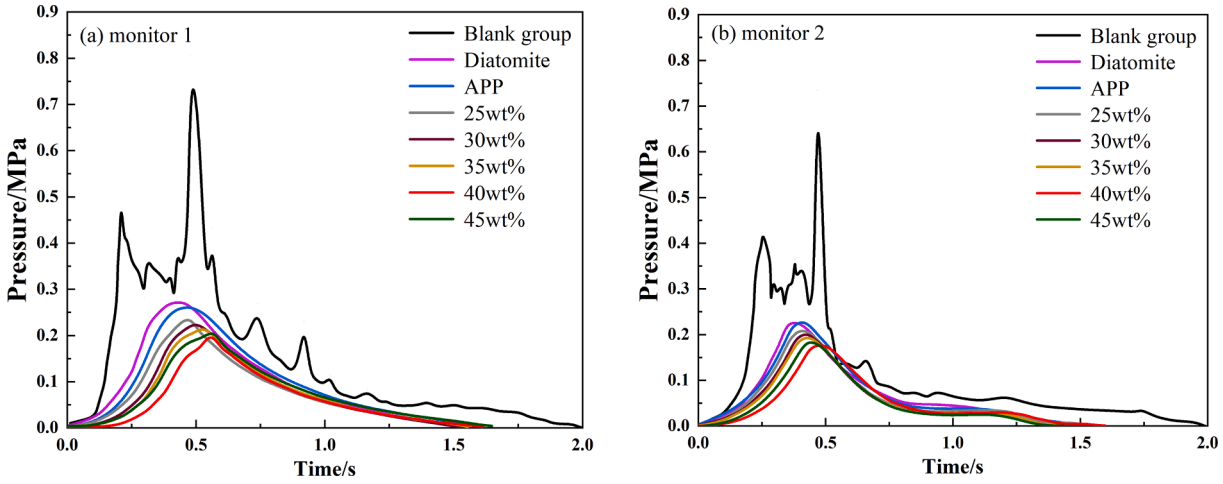

Fig. 5. Overpressure time history curve of different compound ratio suppressors at monitoring point 1 and monitoring point 2.

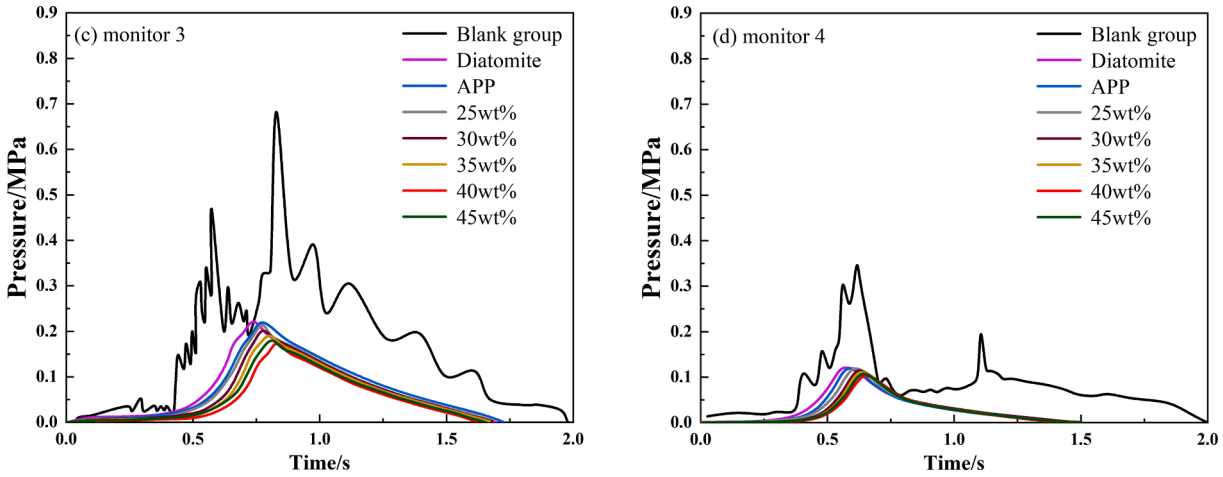

Fig. 6. Overpressure time history curve of different compound ratio suppressors at monitoring point 3 and monitoring point 4.

interval between the first overpressure peak and the second overpressure peak at monitoring point 3 and monitoring point 4 in branch pipe 2 was extended compared to monitoring point 1 and monitoring point 2. The main reason was that the location of monitoring point 1 and monitoring point 2 was close to the source of the explosion, the temperature of the explosion was higher, and the high temperature near the source of the explosion could be transferred to the location of monitoring point 1 and monitoring point 2 more quickly to provide a heat source for the secondary explosion of monitoring point 1 and monitoring point 2. It took some time for the heat source to conduct monitoring point 3 at the right-angle pipe bends and monitoring point 4 near the bursting vents. As a result, the time interval between the occurrence of the first overpressure peak and the second overpressure peak at monitoring point 3 and monitoring point 4 in branch 2 had lengthened. The location also led to a prolonged time to peak overpressure at monitoring points 3 and 4, and the violent reaction was mainly concentrated in the middle of the explosion.

After adding the explosion inhibitor, coal dust, and methane secondary explosion characteristics disappeared, monitoring point 3 and monitoring point 4 at different compound ratios of the overpressure time curve trend were similar, showing a single peak characteristics of the overpressure time curve were more gentle fluctuations, compared to the blank group of the overpressure peak value decreased significantly and peak time increased significantly. Monitoring point 3 overpressure was fully suppressed by 1.75 s and monitoring point 4 overpressure was fully suppressed by 1.5 s. Monitoring point 4 overpressure peak than monitoring point 3 overpressure peak was lower, monitoring point 4 overpressure can be suppressed earlier mainly due to the location of monitoring point 4 was close to the explosion release port and the location of the explosion from the source of the more distant, subject to the other pipeline shock wave back to the superposition of the role of the smaller. At the same time, the overpressure shockwave flowed through monitoring point 4, passing through the bifurcation of the pipeline as well as being subjected to oxygen consumption, resulting in a more significantly suppressed overpressure in monitoring point 4 compared to monitoring point 3.

A comparison of the addition of single-component explosion suppressant found that the addition of APP overpressure peak was slightly smaller than the addition of diatomite overpressure peak, and the addition of APP overpressure peak came later than the diatomite explosion suppressant, composite powder overpressure peak was lower than a single component of the explosion suppressant. In monitoring point 3, the peak overpressure of 25 wt%, 30 wt%, 35 wt%, 40 wt%, and 45 wt% of the compounded explosion suppressant was 0.226 MPa, 0.211 MPa, 0.198 MPa, 0.183 MPa and 0.189 MPa, respectively. Compared to the first overpressure peak without detonation suppressant, the decreases was 51.8 %, 55.0 %, 57.8 %, 61.0 %, and 59.7 %, respectively. In monitoring point 4, the peak overpressure of 25 wt%, 30 wt%, 35 wt%, 40 wt%, and 45 wt% of the compounded explosion suppressant was 0.119 MPa, 0.114 MPa, 0.111 MPa, 0.103 MPa, 0.107 MPa, respectively. Compared to the first overpressure peak without detonation suppressant, the decreases was 67.0 %, 68.4 %, 69.3 %, 71.5 %, and 70.4 %, respectively. Therefore, the 40 wt% loading rate of the compound explosive suppressant overpressure peak in monitoring point 3 and monitoring point 4 of the largest decline, the best effect of suppressing overpressure shock wave.

Fig. 7 shows the inhibition effect of inhibitors with different compounding ratios on explosion overpressure in monitoring point 5 and monitoring point 6. As shown in Fig. 7e and f, in the absence of explosive suppressants, the shock wave evolution process at monitoring point 6 was more complex than at monitoring point 5, with more overpressure fluctuations occurring at the later stages of monitoring point 6. The number of overpressure extreme points occurring in monitoring point 6 was more than that in monitoring point 5, mainly because monitoring point 6 was affected by the superposition of overpressure shock waves in other pipelines more than monitoring point 5. After the first overpressure peak, both monitoring points experienced a secondary explosion due to the incomplete methane-coal dust reaction and the resulting high temperature that would trigger the residue reaction again, and the two monitoring points reached the overpressure peak at similar times.

After adding the explosion suppression agent, suppressed the secondary explosion of methane coal dust, similar to other monitoring points, the overpressure time curve had only one peak, after reaching the peak, the overpressure was a decreasing trend, the two monitoring points in about 1.75 s dropped to 0 MPa, the end of the suppression of the explosion of the end of the time was not much different. However, the location of monitoring point 6 was closer to the source of the explosion compared to the location of monitoring point 5, so the peak overpressure after the addition of the detonation suppression agent monitoring point 6 came earlier than monitoring point 5.

A comparison of the addition of single-component explosion suppressant found that the addition of APP overpressure peak was slightly smaller than the addition of diatomite overpressure peak, and the addition of APP overpressure peak came later than the diatomite explosion suppressant, composite powder overpressure peak was lower than a single component of the explosion suppressant. In monitoring point 5, the peak overpressure of 25 wt%, 30 wt%, 35 wt%, 40 wt%, and 45 wt% of the compounded explosion suppressant was 0.187 MPa, 0.183 MPa, 0.170 MPa, 0.151 MPa and 0.160 MPa, respectively. Compared to the first overpressure peak without detonation suppressant, the decreases was 54.8 %, 55.8 %, 59.0 %, 63.5 %, and 61.3 %, respectively. In monitoring point 6, the peak overpressure of 25 wt%, 30 wt%, 35 wt%,

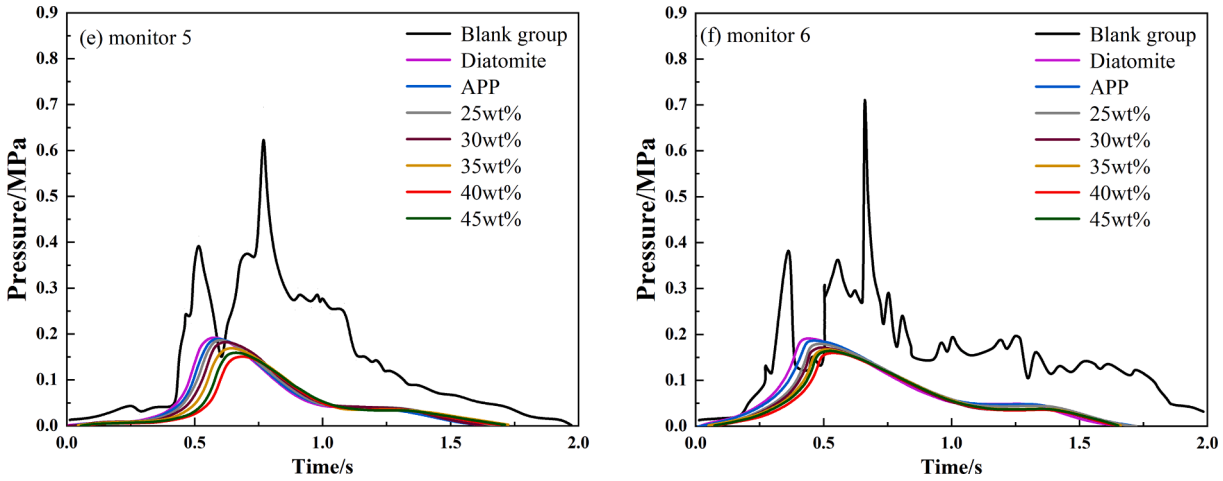

Fig. 7. Overpressure time history curve of different compound ratio suppressors at monitoring point 5 and monitoring point 6.

40 wt%, and 45 wt% of the compounded explosion suppressant was 0.180 MPa, 0.172 MPa, 0.168 MPa, 0.160 MPa and 0.165 MPa, respectively. Compared to the first overpressure peak without detonation suppressant, the decreases was 52.8 %, 55.0 %, 56.0 %, 58.2 %, and 56.9 %, respectively. Therefore, the 40 wt% loading rate of the compound explosive suppressant overpressure peak in monitoring point 5 and monitoring point 6 of the largest decline, the best effect of suppressing overpressure shock wave.

Fig. 8 shows the inhibition effect of inhibitors with different compounding ratios on explosion overpressure in monitoring point 7 and monitoring point 8. As shown in Fig. 8g and h, in the absence of explosive suppressants, the two monitoring points in the branch pipe 4 reached the first overpressure peak due to the action of the forward shock wave, followed by a second overpressure peak in the two monitoring points. Monitoring point 7 of the second overpressure peak was greater than the first overpressure peak, mainly due to the lifted coal dust cloud of coal dust under the action of high temperature and high-pressure thermal decomposition, the production of a sufficient number of combustible gases and participating in the reaction, resulting in the value of the overpressure increases again. However, the second overpressure peak at monitoring point 8 was significantly lower compared to the first overpressure peak. The main reason was that monitoring point 8 was raised by the concentration of coal dust cloud reduced, and monitoring point 8 was in the explosion relief port, part of the pressure loss, and due to the decreasing oxygen content in the pipeline, resulting in a reduction in the power of the secondary explosion, which led to the monitoring of the second overpressure peak at point 8 compared to the first overpressure peak was low.

After adding the inhibitor, the secondary explosion of gas and coal dust at the two monitoring points was suppressed, and similar to the other monitoring points, the overpressure time-course curves showed the characteristic of a “single peak”. At monitoring point 7, about 1.75 s, the explosion overpressure was completely suppressed, at monitoring point 8, about 1.6 s, the explosion overpressure dropped to 0 MPa, monitoring point 8 by the location of the impact of the peak overpressure, resulting in lower peak overpressure, and thus suppression of the peak overpressure after the explosion was also lower, suppression of the explosion used for a shorter period.

A comparison of the addition of single-component explosion suppressant found that the addition of APP overpressure peak was slightly smaller than the addition of diatomite overpressure peak, and the addition of APP overpressure peak came later than the diatomite explosion suppressant, composite powder overpressure peak was lower than a single component of the explosion suppressant. In monitoring point 7, the peak overpressure of 25 wt%, 30 wt%, 35 wt%, 40 wt%, and 45 wt% of the compounded explosion suppressant was 0.235 MPa, 0.222 MPa, 0.213 MPa, 0.200 MPa and 0.208 MPa, respectively. Compared to the first overpressure peak without detonation suppressant, the decreases was 50.4 %, 53.1 %, 55.1 %, 57.8 %, and 56.1 %, respectively. In monitoring point 8, the peak overpressure of 25 wt%, 30 wt%, 35 wt%, 40 wt%, and 45 wt% of the compounded explosion suppressant was 0.153 MPa, 0.149 MPa, 0.146 MPa, 0.135 MPa,

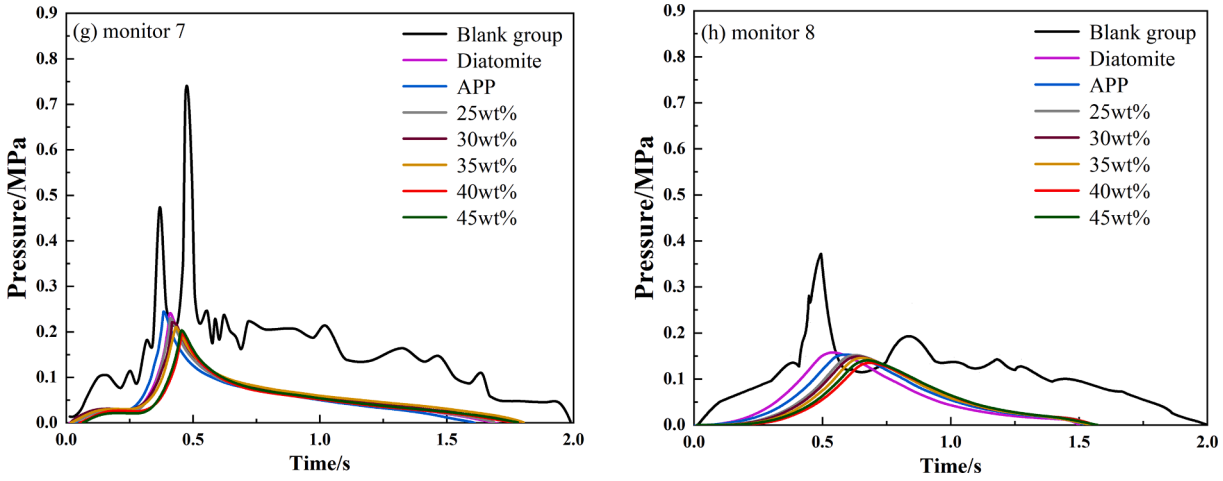

Fig. 8. Overpressure time history curve of different compound ratio suppressors at monitoring point 7 and monitoring point 8.

0.141 MPa, respectively. Compared to the first overpressure peak without detonation suppressant, the decreases was 59.0 %, 60.0 %, 60.6 %, 63.6 %, and 62.12 %, respectively. Therefore, the 40 wt% loading rate of the compound explosive suppressant overpressure peak in monitoring point 7 and monitoring point 8 of the largest decline, the best effect of suppressing overpressure shock wave.

From the above experimental results: whether it was a single-component explosion suppressant or a multi-component composite powder explosion suppressant, both can suppress the secondary explosion of methane-coal dust. The main reason was that the explosion suppressant raised during the explosion suppression process diluted the concentration of coal dust and oxygen, making the coal dust not reach the conditions for the secondary explosion. After adding the explosive suppressant, the overpressure time history curves exhibit a "single peak" characteristic. This change primarily results from the suppressant inhibiting the forward propagation of the explosive shock wave, it reduces the instances of shock wave reflections against the pipeline walls and diminishes the influence of opposing overpressure shock waves from other lines. Consequently, the multiple oscillations formed by oppositely propagating shock waves are also diminished, leading to a significant decrease in the peak overpressure values at various monitoring points. Thus, after the addition of the suppressant, multiple peak overpressures disappear, and the overpressure time history curves show a "single peak" characteristic.

Through the above analysis, it is concluded that: adding an APP explosion suppressor is better than adding a diatomite explosion suppressor to inhibit shock wave explosion overpressure. The composite powder has a synergistic inhibition effect on methane-coal dust explosion shock wave propagation. Among them, 40 wt% loading of the compound explosive suppressant inhibition of overpressure shock wave is the most effective. The maximum reduction in peak explosion overpressure for the 40 wt% loaded composite suppressant is 71.5 % at monitoring point 4.

In addition, the data summarized in Fig. 9 reveals that the maximum pressure at Monitoring Point 1 before the explosion suppression was 0.493 MPa. Monitoring Point 7 followed with a pressure of 0.474 MPa, indicating that the pressure at Point 7 is less than that at Point 1. After the suppression, the explosive pressure pattern remained consistent. The reason lies in the shock wave's behavior as it passes through monitoring point 7. Due to the bifurcation in the pipeline, the shock wave experiences attenuation. Consequently, the pressure loss is greater at this point compared to monitoring point 1. Therefore, the pressure measurements at point 7, both before and after the detonation, remain lower than those

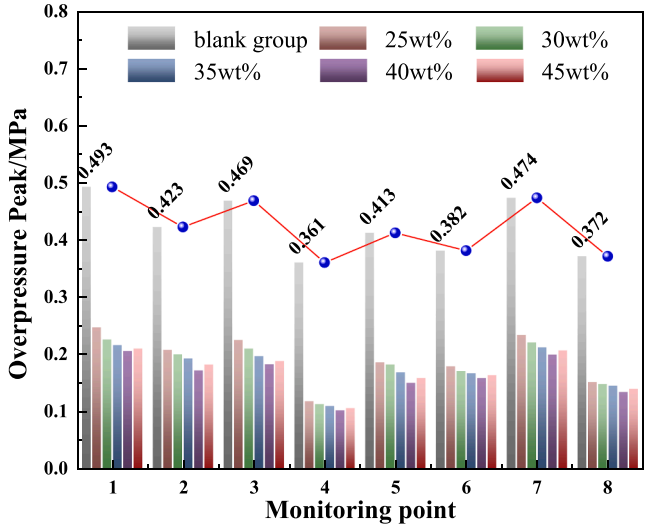

Fig. 9. Peak value of overpressure before and after explosion suppression at each monitoring point.

at point 1. Monitoring points 4 and 8 exhibited the lowest explosion pressure. After suppression, they displayed the same pattern. The reason lies in their locations; they are the farthest from the explosion source and closest to the vent. Consequently, the pressure at points 4 and 8, both before and after suppression, remained lower than at other monitoring points. The pressure at the three monitoring points before and after the suppression is greater than the pressure at point two. Due to the geometric changes of the pipeline, shock waves flowing through right-angled pipes will cause dramatic changes in fluid dynamics. This phenomenon creates a zone of overpressure, resulting in pressures at the three monitoring points being consistently higher than that at point two. The analysis concludes that, unlike the behavior observed in long straight pipes or spherical explosions, shock waves do not simply diminish with distance in various pipe structures. Instead, they exhibit multiple instances of overpressure fluctuations, increasing and decreasing repeatedly during propagation. Therefore, the conclusions obtained from the explosion suppression experiment in the pipe network are more universal.

3.2. *Flame velocity*

Fig. 8 shows the peak flame propagation velocity of diatomite, APP, and different compound ratios of suppressors in branch pipe 1 to branch pipe 4 and the curve of the time to reach the peak flame propagation velocity. The peak flame propagation velocity of the blank group in branch pipe 1 to branch pipe 4 was 348.7 $m{\cdot}s^{-1}$, 368.1 $m{\cdot}s^{-1}$, 385.6 $m{\cdot}s^{-1}$, 342.6 $m{\cdot}s^{-1}$, respectively. From branches 1 to 4 in the figure, it can be seen that the addition of diatomite and APP can significantly reduce the flame propagation speed, and APP had a better effect on flame propagation speed. It can be found that, compared with the condition of the blank group, the peak flame propagation velocity showed a decreasing trend with the increase of the composite powder compound ratio. The peak flame propagation velocities of 25 wt%, 30 wt %, 35 wt%, 40 wt% and 45 wt% compound suppressors in branch pipe 1 was 37.1 $m{\cdot}s^{-1}$, 34.3 $m{\cdot}s^{-1}$, 33.0 $m{\cdot}s^{-1}$, 28.9 $m{\cdot}s^{-1}$ and 30.8 $m{\cdot}s^{-1}$, respectively. The decreases was 89.4 %, 90.2 %, 90.5 %, 91.7 %, and 91.2 % respectively. The peak flame propagation velocities of 25 wt%, 30 wt%, 35 wt%, 40 wt% and 45 wt% compound suppressors in branch pipe 2 was 38.8 $m{\cdot}s^{-1}$, 36.3 $m{\cdot}s^{-1}$, 35.9 $m{\cdot}s^{-1}$, 30.1 $m{\cdot}s^{-1}$ and 33.2 $m{\cdot}s^{-1}$, respectively. The decreases was 88.9 %, 89.6 %, 89.7 %, 91.4 %, and 90.5 %, respectively. The peak flame propagation velocities of 25 wt%, 30 wt%, 35 wt%, 40 wt% and 45 wt% compound suppressors in branch pipe 3 was 42.6 $m{\cdot}s^{-1}$, 40.1 $m{\cdot}s^{-1}$, 38.3 $m{\cdot}s^{-1}$, 33.2 $m{\cdot}s^{-1}$ and 35.9 $m{\cdot}s^{-1}$, respectively. The decreases was 89.0 %, 89.6 %, 90.1 %, 91.4 %, and 90.7 %, respectively. The peak flame propagation velocities of 25 wt%, 30 wt%, 35 wt%, 40 wt% and 45 wt% compound suppressors in branch pipe 4 was 36.5 $m{\cdot}s^{-1}$, 35.9 $m{\cdot}s^{-1}$, 34.2 $m{\cdot}s^{-1}$, 26.8 $m{\cdot}s^{-1}$ and 29.5 $m{\cdot}s^{-1}$, respectively. The decreases was 89.3 %, 89.5 %, 90.0 %, 92.2 %, and 91.4 %, respectively. Among them, the flame propagation velocity of 40 wt% composite powder in each branch pipe decreased the most.

According to the above experimental results, the effect of APP on flame propagation of gas-coal dust explosion is better than that of diatomite, and the composite powder has a synergistic effect on flame propagation of methane-coal dust explosion. Among them, the compound powder of 40 wt% has the best effect of inhibiting the spread of explosion flame. The peak flame propagation velocity of 40 wt% composite powder in branch pipe 1, branch pipe 2, branch pipe 3, and branch pipe 4 decreased by 91.7 %, 91.4 %, 91.4 %, and 92.2 % respectively, and the largest decrease was 92.2 % in branch pipe 4.

In addition, in terms of flame wave velocity, it can be seen from Fig. 10 that the order of flame propagation velocity before explosion suppression is branch pipe 3, branch pipe 2, branch pipe 1, branch pipe 4. After explosion suppression, the propagation velocity of each branch pipe flame wave is the same as that before explosion suppression. The flame wave velocity in branch pipe 3 was the largest because the

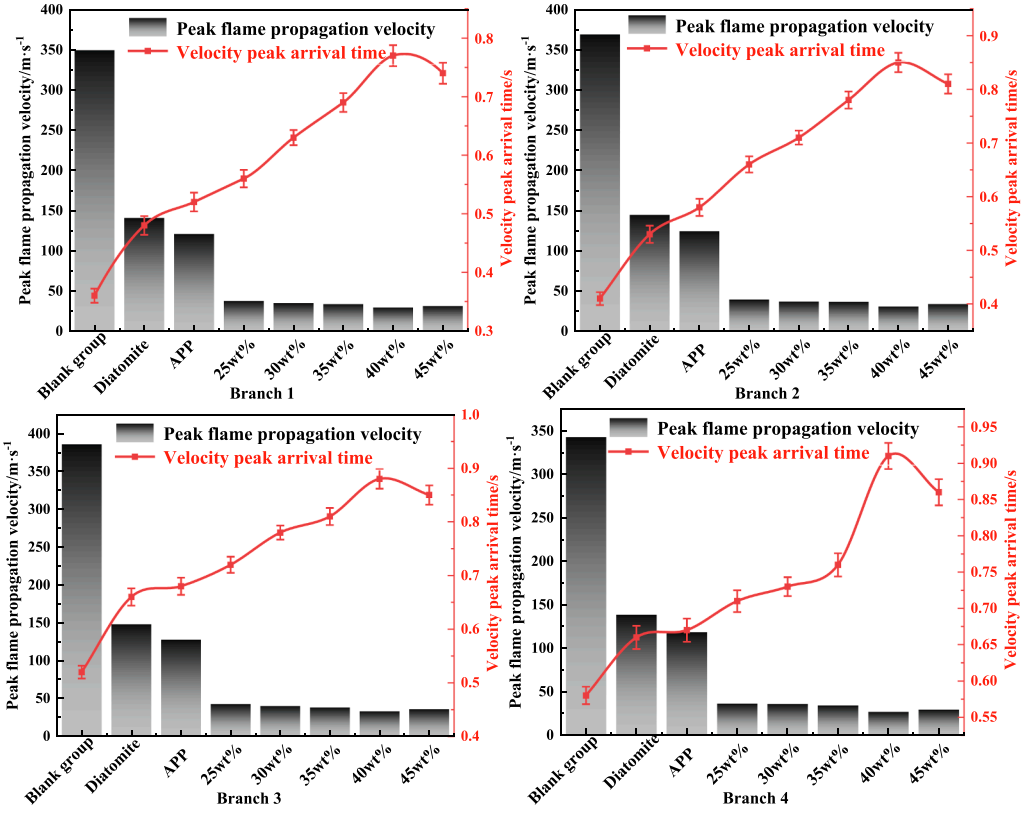

Fig. 10. Inhibition effect of different compound ratio inhibitors on flame velocity.

pressure loss at monitoring points 3 and 4 in branch pipe 3 was the largest. The flame front acceleration gradient in branch pipe with greater pressure loss was larger and the flame front propagation speed was higher, while the flame front acceleration gradient in branch pipe with smaller pressure loss was smaller and the flame front velocity was lower. Therefore, according to the different structures of the pipeline, the flame wave propagation speed will increase and decrease with the change in the pipeline. Therefore, the conclusions obtained from the explosion suppression experiment in the pipeline network are more universal. In the future, explosion prevention and control can be carried out in specific locations according to the geometric mechanism of the actual pipe network, which provides an effective means for ensuring the safe operation and emergency rescue of the pipeline system.

4. Discussion

The methane-coal dust explosion inhibition experiments showed that the 40 wt% composite powder had a significant inhibition effect on methane-coal dust explosion. The inhibition mechanism was analyzed in the following three aspects: pyrolysis properties, explosive residue, and chain reaction (Hou et al., 2023; Wei et al., 2021).

The pyrolytic properties of diatomite, APP, and diatomite-APP composite powder were tested at a temperature increase rate of 10 K/min, a temperature range of 25–800 °C, and a nitrogen atmosphere, and the thermogravimetric (TG) and differential scanning calorimetry (DSC) curves are shown in Fig. 11.

Fig. 11a shows the APP pyrolysis curve. First, APP had a mass loss of 1.8 % through water evaporation. APP at about 136.4–233.9 °C to pyrolyze to ammonium phosphate and ammonia gas, the maximum heat absorption peak corresponded to a temperature of about 229.5 °C, the rate of weightlessness during this period was approximately 41.2 %. Then, between 233.9 °C and 607.5 °C, APP pyrolysis continued to pyrolyze to form phosphoric acid and ammonia gas. Finally, the residual amount of APP after pyrolysis was 28.4 %. The thermal decomposition

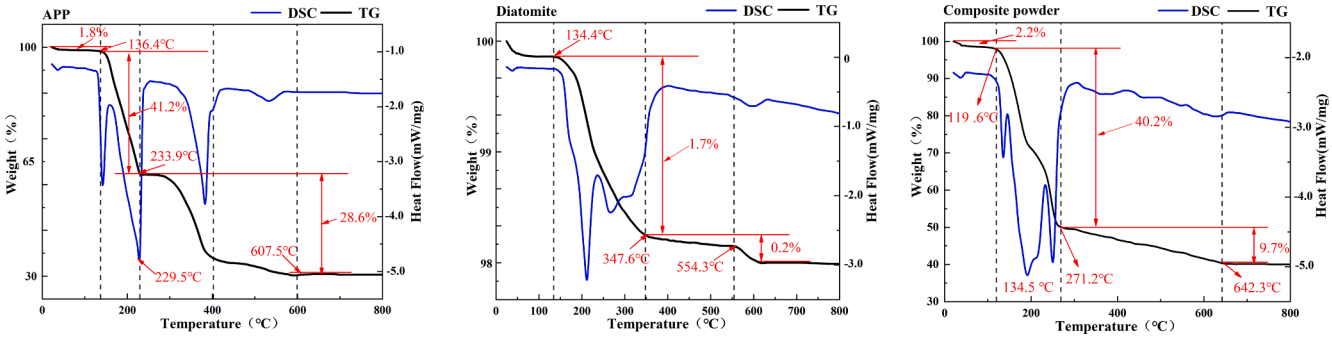

(a) APP pyrolysis curve. (b) Pyrolysis curve of diatomite (c) App-diatomite pyrolysis curve.

Fig. 11. TG-DSC curves of explosion inhibitors.

of APP occurred mainly in the form of a heat-absorption reaction, producing NH_3 gas, water vapor, phosphoric acid, and other phosphorus oxides.

In Fig. 11b, the mass loss of diatomite was 2.0 %. Diatomite mass loss was mainly in the range of 134.4–347.6 °C. As shown in Fig. 12, there were many silica hydroxyl groups on the surface of silica particles, and under the high-temperature heat treatment conditions of methane-coal dust explosion, with the increase of temperature in the pipeline, the hydrogen-bonded hydroxyl groups and isolated hydroxyl groups undergo condensation dehydroxylation(He et al., 2022; Luo et al., 2016). It was inferred from the surface hydroxyl removal law of silica under heat treatment conditions that the mass loss of diatomaceous earth at 134.4–347.6 °C was mainly caused by physically adsorbed water, desorption of water bound to hydroxyl hydroxyls with hydrogen bonding, and condensation and dehydration of some of the hydrogen-bonded bonding hydroxyls and a few of the isolated hydroxyls. The weight loss phase after 554.3 °C was attributed to the destruction of the diatomite structure.

Fig. 11c shows the pyrolysis curve of diatomite-APP composite powder. The initial weight loss temperature of the composite powder (119.6 °C) was lower than that of the diatomite and APP due to the increase in the surface energy of the monomer after treatment with the diatomite-APP composite powder. The weight loss of the composite powder occurred in two stages. The first stage (119.6–271.2 °C) was caused by evaporation of water and pyrolysis of APP. The second stage (271.2–642.3 °C) corresponded to the destruction of the structure of the diatomaceous earth. The total mass loss for both phases was 59.8 %. It can be seen that the rate of weight loss from the heat of the composite powder was significantly lower than the rate of weight loss from the heat of the APP. Meanwhile, it can be seen from the DSC curve that the composite powder had an obvious heat absorption peak at 134.5 °C with a heat absorption of 634.82 J/g. It exceeded the weighted average of heat absorption between 25 and 800 °C for APP and diatomaceous earth (~548.79 J/g). Therefore, the composite powder inhibitor had a synergistic effect.

After the methane/coal dust explosion, there were still many residues, which were characterized chemically by X-ray photoelectron spectroscopy (XPS). Fig. 13 shows the XPS survey spectra of the residual samples after the coal dust explosion. In Fig. 13, condition 1, condition 2, and condition 3 are the raw coal, the products after the explosion of the raw coal, and the products after the explosion of the coal dust with the addition of the composite powder, respectively. It can be seen that there are characteristic elemental peaks of C, O, N, P, Si, and Al in the coal dust residue, of which N and P belong to APP or APP decomposition products, and Si and Al belong to diatomite or diatomite decomposition products. As can be seen from the figure, the intensity of the C elemental content in the explosive residue after the addition of the composite powder increased, while the O elemental content increased significantly.

The C 1s and O 1s spectra were fitted, as shown in Fig. 14. The C 1s chemical bonds of residue samples after the explosion, mainly including C—C, C—O, C═O and C—H, which appeared respectively near 286.1 eV, 286.3 eV, 289.1 eV和287.4 eV, as shown in Fig. 14a. Fig. 14b showed the C-element spectra of the coal dust explosion products with the addition of composite powder, from which it can be seen that the

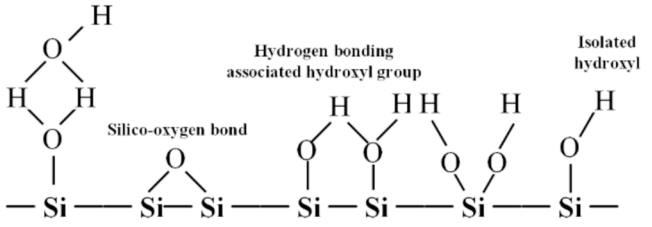

Fig. 12. Surface hydroxyl species of silicon dioxide.

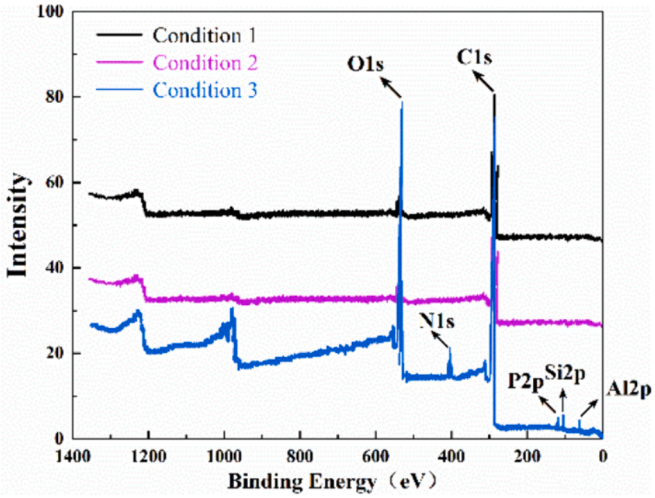

Fig. 13. XPS survey spectra of residue samples.

C—C content increased significantly compared with that in Fig. 14a, indicating that the addition of composite powder slowed down the decomposition of C-element in coal dust. Fig. 14c showed the O-element spectra of the coal dust explosion products without composite powder, and Fig. 14d showed the O-element spectra of the coal dust explosion products with composite powder. As can be seen from Fig. 14d, in the explosion residue with composite powder, O1s mainly existed in the form of C═O/P═O and C—O/P—O—P/Si—O—Si in the cinder, and the higher O content in the explosion residue with composite powder indicated that there were enough volatile components that had not been released. It has been shown that oxygen-containing functional groups have a significant effect on the properties of coal, and the oxygen content of coal decreases with the decrease of volatile components. It can be seen that the addition of composite powder inhibits the precipitation of volatile components in coal dust and reduces the intensity of coal dust explosion.

Fig. 15 shows the APP-diatomite composite powder explosion suppression mechanism. It can be seen through the explosion suppression mechanism diagram, that during the reaction process APP decomposition of NH_2-radicals can be further reacted with H-, HO-radicals, which can continue to promote the consumption of H-, HO-radicals and oxygen, to inhibit the methane coal dust mixture explosion. At the same time, APP decomposition produces a large number of non-combustible gases (such as NH_3, H_2O, etc.) that can dilute the oxygen in the air, reduce the concentration of combustible gases, while the evaporation of water vapor would take away the heat in the explosion, thereby reducing the temperature of the explosion environment, slowing down the explosion rate.

Composite powder in the diatomite has a porous structure, porosity of 90–92 %, with a large specific surface area, high activity, rapid thermal decomposition, radiation reflection of the strong surface, strong adsorption properties, can be adsorbed in the pipeline by the explosion raised by the incomplete reaction of the coal dust, reduce the concentration of coal dust in the pipeline, to reduce the chances of generating a secondary explosion. It had a high free radical capture capacity, the porous structure of diatomite can adsorb free radicals and oxygen in the explosive chain reaction process, thereby reducing the free radical collision rate, playing a role in reducing the explosion reaction rate, and then inhibit the methane-coal dust explosion intensity.

5. Conclusions

In this paper, using diatomite as the carrier, ammonium polyphosphate (APP) was compounded with diatomite, and the inhibition effects of APP, diatomite, and APP-diatomite compounded powders on

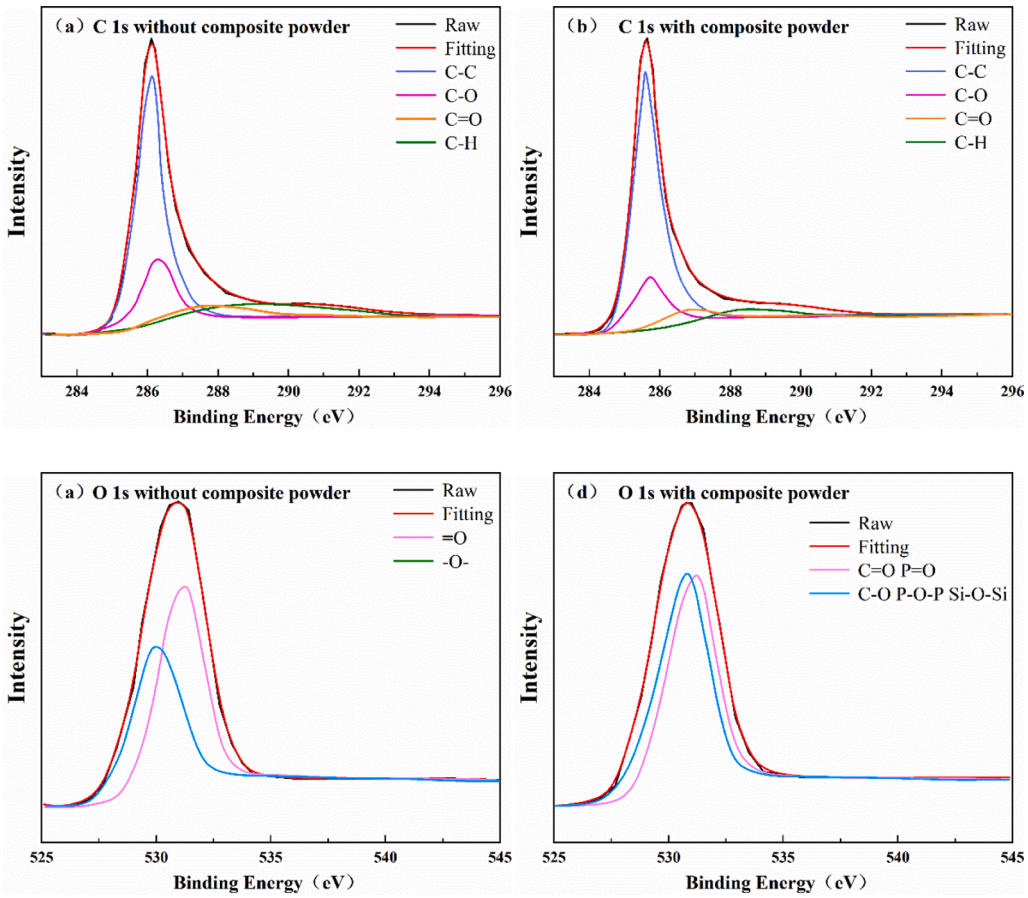

Fig. 14. XPS spectra of coal dust explosion products.

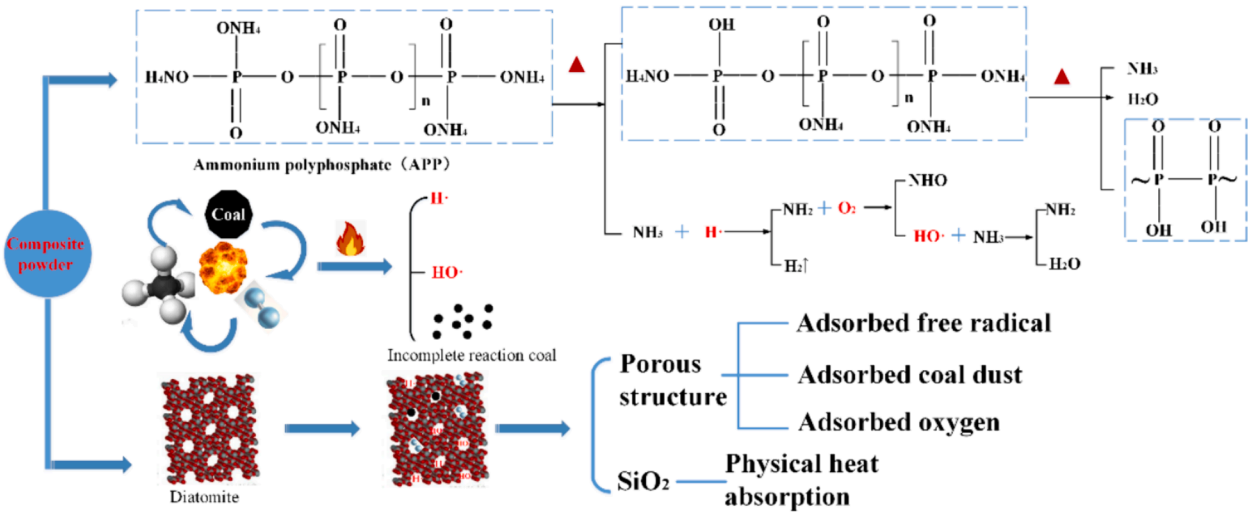

Fig. 15. APP-diatomite composite powder explosion suppression mechanism diagram.

the methane/coal dust composite explosions were investigated in the self-constructed pipeline network experimental system, and the main conclusions are as follows:

1. By scanning electron microscopy and X-ray photoelectron spectroscopy, it is found that the APP powder is uniformly distributed on the porous mesh structure of diatomite, and the diatomite in the composite powder not only made up for the defects of APP without porosity but also improves the phenomenon that the monomer APP is easy to be agglomerated and cohesive.
2. APP, diatomite, and composite powder have inhibited the secondary explosion of methane/coal dust, composite powder is better than a single powder explosion suppression ability. When the APP loading on the surface of diatomite is 40 wt%, composite powder has the best effect on explosion suppression, with the peak maximum explosion overpressure and the peak maximum flame propagation velocity reduced by 71.5 % and 92.2 %, respectively.

3. The explosion suppression mechanism of APP-diatomite composite powder is analyzed through three aspects: pyrolysis properties, explosive residue, and chain reaction. The synergistic inhibition of methane coal dust composite explosion by APP-diatomite composite powder is mainly reflected in heat absorption, inerting, dilution, adsorption of free radicals, and free radical binding.
4. The experimental conclusions obtained in the pipe network are similar but not exactly the same as those obtained in the long straight pipe or spherical explosion. According to the different structures of the pipe, the shock wave and flame wave do not gradually decrease with the increase of distance when propagating, but will repeatedly increase or decrease the overpressure and the flame propagation speed in different branch pipes will be different. Therefore, the conclusions obtained from the explosion suppression experiment in the pipeline network are more universal. In the future, explosion prevention and control can be carried out in specific locations according to the actual geometric mechanism of the pipeline network, which provides an effective means for ensuring the safe operation of the pipeline system and emergency rescue.

CRediT authorship contribution statement

Jinzhang Jia: Writing – review & editing. **Xiuyuan Tian:** Writing – review & editing.

Declaration of competing interest

The authors declare that they have no known competing financial interests or personal relationships that could have appeared to influence the work reported in this paper.

Acknowledgements

This work was partly supported by the National Natural Science Foundation of China (grant number 52174183).

This work was partly supported by the National Natural Science Foundation of China (grant number 52374203).

References

Ajrash, M.J., Zanganeh, J., Moghtaderi, B., 2016. Methane-coal dust hybrid fuel explosion properties in a large scale cylindrical explosion chamber. J. Loss Prev. Process Ind. 40, 317–328.

Bihe, Yuan, Hongji, Tao, Yaru, Sun, et al., 2021. Study on synergistic suppression of methane explosion by porous mineral materials-ammonium polyphosphate composite powder. China Saf. Sci. J. 31 (03), 41–46.

Cao, Xingyan, Wei, Haoyue, Wang, Zhirong, et al., 2023. Experimental research on the inhibition of methane/coal dust hybrid explosions by the ultrafine water mist. Fuel 331, 125937.

Cao, Xingyan, Wang, C., Wang, Yue, et al., 2024. Research on the inhibition characteristics of ultrafine water mist on gas/dust two-phase mixture explosions. Fuel 357, 129967.

Chen, Di, Wu, Chengqing, Li, Jun, et al., 2023. An overpressure-time history model of methane-air explosion in tunnel-shape space. J. Loss Prev. Process Ind. 82, 105004.

Cheng, Fangming, Deng, Jun, Luo, Zhenmin, et al., 2010. Experimental study on inhibiting gas explosion using diatomite powder. J. Min. Saf. Eng. 27 (04), 604–607.

Dai, Huaming, Liang, Guangqian, Yin, Hepeng, et al., 2022. Experimental investigation on the inhibition of coal dust explosion by the composite inhibitor of carbamide and zeolite. Fuel 308, 121981.

Dong, Zhangqiang, Liu, Lijuan, Chu, Yanyu, et al., 2022. Explosion suppression range and the minimum amount for complete suppression on methane-air explosion by heptafluoropropane. Fuel 328, 125331.

Duan, Yulong, Long, Fengying, Huang, Jun, et al., 2022. Effects of porous materials with different thickness and obstacle layout on methane/hydrogen mixture explosion with low hydrogen ratio. Int. J. Hydrogen Energy 47 (63), 27237–27249.

Dunn-Rankin, D., McCann, M.A., 2000. Overpressures from nondetonating, baffle-accelerated turbulent flames in tubes. Combust. Flame 120 (4), 504–514.

Gieras, M., Klemens, R., Rarata, G., et al., 2015. Determination of explosion parameters of methane-air mixtures in the chamber of 40 dm^3, at normal and elevated temperature. J. Loss Prev. Process Ind. 15 (03), 263–270.

Guo, Rui, Xu, Chen, Li, Nan, et al., 2024. Suppression effect of nanocomposite inhibitor on Methane-Coal dust explosion flame propagation. Adv. Powder Technol. 35 (1), 104314.

He, Wenhao, Hao, Chaoyu, Zhang, Yachao, et al., 2022. Microscopic mechanism analysis of inhibition on methane explosion by diatomite. J. China Coal Soc. 47 (10), 3695–3703.

Hou, Zhenhai, Wang, Biao, Zhu, Yunfei, 2023a. Experimental study on pressure wave-induced explosion of different types of deposited coal dust. Process Saf. Environ. Prot. 172, 825–835.

Hou, Zhenhai, Wang, Deming, Luo, Shengyun, et al., 2023b. Study on flame propagation characteristics of deposited coal dust explosion induced by pressure waves of different intensities. Fire Mater. 47 (8), 1043–1052.

Jiang, Haipeng, Bi, Mingshu, Huang, Lei, et al., 2022. Suppression mechanism of ultrafine water mist containing phosphorus compounds in methane/coal dust explosions. Energy 239, 121987.

Liu, Aihua, Lu, Xiner, Zhou, Xinying, et al., 2023. Experimental investigation on suppression of methane explosion using $KHCO_3$/zeolite composite powder. Powder Technol. 415, 118157.

Long, Fengying, Duan, Yulong, Yu, Shuwei, et al., 2022. Effect of porous materials on explosion characteristics of low ratio hydrogen/methane mixture in barrier tube. J. Loss Prev. Process Ind. 80, 104875.

Luo, Zhenmin, Cheng, Fangqin, Wang, Tao, et al., 2016. Suppressive effects of silicon dioxide and diatomite powder aerosols on coal mine gas explosions in highlands. Aerosol Air Qual. Res. 16 (9), 2119–2128.

Moiseeva, K.M., Krainov, A.Y., 2023. Distinctive features of propagation of the flame of a coal–methane–air mixture in a cylindrical channel. J. Eng. Phys. Thermophys. 96 (4), 913–921.

Pearce, J.K., Hofmann, H., Baublys, K., et al., 2023. Sources and concentrations of methane, ethane, and CO2 in deep aquifers of the Surat Basin, Great Artesian Basin. Int. J. Coal Geol. 265, 104162.

Shi, Jingtai, Zhang, Pikai, Xu, Yong, et al., 2023. Effects of dilute coal char particle suspensions on propagating methane detonation wave. Combust. Flame 249, 112618.

Song, Shixiang, Cheng, Yi, Meng, Xiangrui, et al., 2019. Hybrid CH_4/coal dust explosions in a 20-L spherical vessel. Process Saf. Environ. Prot. 122, 281–287.

Sun, Jiahua, Zhao, Yi, Wei, Chunrong, et al., 2011. The comparative experimental study of the porous materials suppressing the gas explosion. Proc. Eng. 26, 954–960.

Wang, Jian, Zhao, Yongxian, Zheng, Ligang, et al., 2022. Study of methane explosion suppression characteristics of N_2 and CO_2 in variable cross-section ducts. ACS Omega 8 (1), 1375–1388.

Wei, Qingxi, Zhang, Yansong, Chen, Kun, et al., 2021a. Preparation and performance of novel APP/NaY-Fe suppressant for coal dust explosion. J. Loss Prev. Process Ind. 69, 104374.

Wei, Xiangrui, Zhang, Yansong, Wu, Guangan, et al., 2021b. Study on explosion suppression of coal dust with different particle size by shell powder and $NaHCO_3$. Fuel 306, 121709.

Yu, Minggao, Wang, Fengchuan, He, Tongchuan, et al., 2023. Experimental exploration and mechanism analysis of the deflagration pressure of methane/pulverized coal blenders inhibited by modified kaoline-containing compound inhibitors. Fuel 333, 126353.

Yu, Minggao, Wang, Fengchuan, Li, Haitao, et al., 2024. Macroscopic behaviors and chemical reaction mechanism for the inhibition of $NH_4H_2PO_4$ powder in hybrid methane/coal dust deflagrations. Fuel 356, 129558.

Zhao, Qi, Chen, Xianfeng, Li, Yang, 2022a. Suppression mechanisms of ammonium polyphosphate on methane/coal dust explosion: based on flame characteristics, thermal pyrolysis and explosion residues. Fuel 326, 125014.

Zhao, Tenglong, Chen, Xiaokun, Luo, Zhenmin, et al., 2023. Effect of N_2 inerting on the inhibition of methane explosions by a multicomponent powder. Fuel 337, 127203.

Zhao, Qi, Liu, Jing, Chen, Xianfeng, et al., 2021. Hindrance and suppression characteristics of local whole-inerting zone on flame propagation of methane/coal dust deflagration. Fuel 305, 121483.

Zhao, Qi, Li, Yang, Chen, Xianfeng, 2022b. Fire extinguishing and explosion suppression characteristics of explosion suppression system with N_2/APP after methane/coal dust explosion. Energy 257, 124767.

Zhao, Peng, Tan, Xin, Schmidt, M., et al., 2020. Minimum explosion concentration of coal dusts in air with small amount of CH_4/H_2/CO under 10-kJ ignition energy conditions. Fuel 260, 116401.